

Detection of synthetic RGDS(PO₃H₂)PA peptide adsorption using a titanium surface plasmon resonance biosensor

Yasuhiko Abe · Kyou Hiasa · Isao Hirata · Yohei Okazaki ·
Keisuke Nogami · Wataru Mizumachi · Yasuhiro Yoshida ·
Kazuomi Suzuki · Masayuki Okazaki · Yasumasa Akagawa

Received: 9 September 2010 / Accepted: 19 December 2010 / Published online: 8 January 2011
© Springer Science+Business Media, LLC 2010

Abstract The purpose of this study was to measure the time-dependent chemical interaction between synthetic RGDS(PO₃H₂)PA (P-RGD) peptide and titanium surfaces using a titanium surface plasmon resonance (SPR) biosensor and to determine the degree of peptide immobilization on the surfaces. An SPR instrument for ‘single-spot’ analysis was used for nanometer-scale detection of biomolecular adsorption using a He–Ne laser light according to Knoll’s method. The oxidized titanium surface was etched when exposed to H₃PO₄ solutions with a pH of 2.0 or below. The amount of P-RGD adsorbed at pH 1.9 was approximately 3.6 times as much as that at pH 3.0 ($P < 0.05$). P-RGD naturally adsorbed on the oxidized

titanium surface as a consequence of the bonding and dissociation mechanism of the phosphate functional group. Furthermore, the control of pH played a very important role in the interaction between P-RGD and the surface. These findings show that pH control may promote progressive binding of biomolecules with the phosphate functional group to the titanium surface.

1 Introduction

Controlling the physical and chemical properties of titanium surfaces is of prime importance when developing medical devices and biosensors [1]. Indeed, biomimetic surface modification of titanium implants would enable specific cell–extracellular matrix (ECM) interactions [2–5]. The Arg-Gly-Asp (RGD) peptide sequence is known as a cell recognition site for numerous adhesive proteins present in the ECM and in blood. Whilst surface-immobilized RGD groups enhance cell attachment, RGD components present in solution can effectively inhibit cell attachment by competing with endogenous ligands for the same recognition site [1, 2].

Ferris et al. [6] suggested surface modification with the peptide sequence RGDC using gold-thiol chemistry, since small peptides can be synthesized in very high purity and have bioactivity that is independent of tertiary structure. However, this process is complex and, importantly, the intrinsic biocompatibility of titanium is left unexploited when the surface is gold-coated. Subsequently, Schuler et al. [7] introduced a non-fouling poly(L-lysine)-graft-poly(ethylene glycol) (PLL-g-PEG) molecular assembly system, which allowed exploitation of specific cell–RGD peptide interactions even in the presence of serum. They found that osteoblast attachment and footprint areas

Y. Abe (✉) · K. Hiasa · Y. Okazaki · K. Nogami ·
W. Mizumachi · Y. Akagawa
Department of Advanced Prosthodontics,
Division of Cervico-Gnathostomatology,
Graduate School of Biomedical Sciences,
Hiroshima University, 1-2-3, Kasumi, Minami-ku,
Hiroshima 734-8553, Japan
e-mail: abey@hiroshima-u.ac.jp

I. Hirata · M. Okazaki
Department of Biomaterial Science,
Division of Molecular Medical Science,
Graduate School of Biomedical Sciences,
Hiroshima University, 1-2-3, Kasumi, Minami-ku,
Hiroshima 734-8553, Japan

Y. Yoshida · K. Suzuki
Department of Biomaterials, Graduate School of Medicine,
Dentistry and Pharmaceutical Sciences, Okayama University,
2-5-1, Shikata-cho, Kita-ku, Okayama 700-8525, Japan

Y. Yoshida · K. Suzuki
Research Center for Biomedical Engineering,
Okayama University, 2-5-1, Shikata-cho, Kita-ku,
Okayama 700-8525, Japan

increased with the RGD peptide surface density. The potential of such a route was further supported by an *in vivo* study on RGD-coated titanium implants inserted in two bone-gap models, which concluded that RGD peptide coatings can potentially enhance tissue integration [8].

In addition to RGD peptide coatings, phosphate-containing coatings have also been studied. Healy and Ducheyne [9] demonstrated that phosphate has strong affinity for titanium oxide surfaces. Viornery et al. [10] suggested that phosphonic acid molecules that are covalently attached to a titanium surface might form a scaffold for new bone formation, ultimately leading to interfacial bonding between implant and host tissue. Phosphonic acid groups remain strongly bound to titanium oxide surfaces over a large pH range (pH 1–9) and are well distributed over the titanium surface. These properties formed the basis for an easy and practical method employing a new phosphonate-anchor system for coating titanium implants with the α -specific cyclic-RGD peptide [11]. In fact, several biochemical surface modification techniques that are currently being investigated and pursued essentially rely on the idea of chemically bonding small amino acids to titanium surfaces by means of phosphorylation. Abe et al. [12] verified that *o*-phospho-L-threonine formed stable chemical bonds with titanium surfaces treated with HCl [13]. Based on these results, they synthesized a RGDS(PO₃H₂)PA (P-RGD) peptide.

The purpose of this study was to measure the time-dependent chemical interaction between synthetic P-RGD peptides and titanium surfaces using surface plasmon resonance (SPR) biosensor and to determine the degree of peptide immobilization on the surfaces.

2 Materials and methods

2.1 Materials

Phosphonic acid (H₃PO₄; 98.0 mol. wt., Lot No. 24-2610, Katayama Chemical, Osaka, Japan), *o*-phospho-L-threonine (P-Thr; 199.1 mol. wt., Lot No. 074K4023, Sigma-Aldrich, St. Louis, MO, USA) and *o*-phospho-L-serine (P-Ser; 185.1 mol. wt., Lot No. 21K1389, Sigma-Aldrich, St. Louis, MO, USA) were used for the purpose of this study. The peptide sequence P-RGD (681.6 mol. wt., Lot No. 980-410221) was synthesized by Peptide Institute Inc. (Osaka, Japan). The 99.0% purity of the peptide was evaluated by a reversed-phase high-performance liquid chromatography (HPLC; LC8A, Shimadzu, Kyoto, Japan).

2.2 SPR analysis

A titanium surface plasmon resonance (Ti-SPR) biosensor (Osaka Vacuum, Osaka, Japan) was fabricated by the

following means of surface deposition under 2.0×10^{-2} Pa using an electron-beam evaporation method: surface coating with a 1-nm Cr film on an S-LAL10 glass plate (diameter: 15.0 mm, thickness: 1.0 mm, refractive index: 1.72; Artech Associates, Kyoto, Japan), followed by additional deposition of a 49-nm sensing layer with Au. A 5-nm Ti sensing film was then formed on the SPR biosensor.

The SPR is commonly used for nanometer-scale detection of protein–protein interactions, molecular adsorption, and surface structure changes, using a He–Ne laser light, Knoll's method [14], and the Kretschmann configuration [15]. The SPR instrument for 'single-spot' analysis [16, 17] was constructed by referring to Knoll's method [14]. The Ti-SPR biosensor was coupled to an equilateral triangle prism (refractive index: 1.72; S-LAL10, Artech Associates, Kyoto, Japan) with an index matching fluid (refractive index: 1.72; Certified Refractive Index Liquids Series M, Lot No. NJ07009, Cargille Laboratories, Cedar Grove, NJ, USA). The He–Ne laser light (632.8 nm) was linearly *p*-polarized using a Gran-Thomson prism and was focused on the sample through the equilateral triangle prism. The intensity of the reflectance was measured by scanning a photo-diode detector through the angles and processing the data by a computer. The Ti-SPR biosensor was mounted on an SPR flow cell. Milli-Q water was allowed to flow across the Ti surface at 2.5 ml/min for 1 min, after which the SPR adsorption profile was recorded during the flowing of H₃PO₄ (pH 3.0, 2.0, 1.9, or 1.8), 50 mM P-Thr (pH 2.0), 50 mM P-Ser (pH 1.9), 5 mM P-RGD peptide (pH 3.0 or 1.9), respectively, for 20 min. After reaching equilibrium, the flow cell was washed with MilliQ water for 19 min. All experiments were carried out at 25°C.

Depending on the refractive index of the sensing layer, the SPR curve of reflectivity versus incidence angle shifts to larger angles as the refractive index of the sensing layer increases, and the incidence angle of minimum reflectivity is called the SPR angle (degree angle: θ_{SPR}). The dependence of the SPR angle shift on changes in the refractive index is determined by multilayer Fresnel reflectivity calculations [18]. In this study, the SPR spectra of the Ti-SPR biosensor were simulated by the Fresnel's law for the multilayer system, S-LAL 10 prism (refractive index: 1.72)/S-LAL 10 glass plate (refractive index: 1.72)/Cr (permittivity: $-30 + 31i$)/Au (permittivity: $-12.5 + 1.25i$)/Ti (permittivity: $-4.3 + 21.1i$)/TiO₂ (permittivity: 5.19)/protein (refractive index: 1.45)/water (refractive index: 1.33), and thus we estimated of the coefficient (4.02 pg/mm²/mDa) to convert the SPR angle shift (mDa) into the protein adsorption (pg/mm²) [18]. Hence the thickness of the molecule layer was calculated from the SPR angle shift. The actual SPR angle shifts of pH 2.0-P-Thr, pH 1.9-P-Ser, and pH 3.0- and

1.9-P-RGD peptide were estimated as differences from the SPR angle shift at the same pH as that of H_3PO_4 as a baseline solution. The amounts of P-Ser, P-Thr and P-RGD adsorption to the Ti-SPR biosensor (pg/mm^2) were calculated from the equation: $4.02 (\text{pg}/\text{mm}^2/\text{mDa}) \times \text{actual SPR angle shift (mDa)}$. The data were expressed as mean \pm standard deviation of five independent measurements for the SPR angle shift at 40 min per experimental solution. The data on the SPR angle shift (mDa) at 40 min for each pH- H_3PO_4 solution, and the data on the actual SPR angle shift (mDa) and the adsorbed amount (pg/mm^2) at 40 min for pH 2.0-P-Thr, pH 1.9-P-Ser, and pH 3.0- and 1.9-P-RGD peptide solution were analyzed using *t*-tests ($P < 0.05$).

3 Results

The SPR angle shifts (mDa) at 40 min for each of the H_3PO_4 solutions at pH values of 3.0, 2.0, 1.9, and 1.8 are shown in Table 1. The SPR angles shifted to a lower angle except for the pH 3.0-solution. The SPR angle shift for the pH 1.8-solution (-125.4 ± 35.8 mDa) was significantly smaller than the shifts for other pH solutions.

Figure 1a shows the 40-min time evolution curves for the Ti-SPR biosensor during pH 2.0-P-Thr adsorption and exposure to pH 2.0- H_3PO_4 as the baseline solution. The actual SPR angle shift at 40 min after exposure to P-Thr was 32.7 ± 12.8 mDa, and the adsorbed amount was 131.5 ± 62.9 pg/mm^2 (Table 2). Figure 1b shows the time evolution curves for the biosensor during pH 1.9-P-Ser adsorption and exposure to pH 1.9- H_3PO_4 as the baseline solution. The actual SPR angle shift at 40 min after exposure to P-Ser was 36.6 ± 9.8 mDa, and the adsorbed amount was 146.9 ± 48.3 pg/mm^2 (Table 2). The values for P-Thr and P-Ser were not statistically different ($P > 0.05$).

Figure 1c shows the time evolution curves for the biosensor during pH 3.0-P-RGD peptide adsorption and exposure to pH 3.0- H_3PO_4 as the baseline solution. The actual SPR angle shift at 40 min after exposure to the pH

3.0-P-RGD peptide was 35.7 ± 22.3 mDa, and the absorbed amount was 143.3 ± 109.9 pg/mm^2 (Table 2). Figure 1d shows the time evolution curves for the biosensor during pH 1.9-P-RGD peptide adsorption and exposure to pH 1.9- H_3PO_4 as the baseline solution. The actual SPR angle shift at 40 min after exposure to pH 1.9-P-RGD peptide was 128.6 ± 40.1 mDa, and the absorbed amount was 517.1 ± 197.4 pg/mm^2 (Table 2). The values for pH 3.0- and pH 1.9-P-RGD peptide were statistically different ($P < 0.05$). The amount of P-RGD peptide adsorbed at pH 1.9 was approximately 3.6 times as much as that at pH 3.0.

4 Discussion

SPR analyses on the chemical interaction between H_3PO_4 solution and a Ti-SPR biosensor clarified that the oxidized Ti surface was etched when exposed to H_3PO_4 solutions with a pH of 2.0 or below. The average changes in thickness at pH values of 2.0, 1.9, and 1.8 were about 20, 50, and 120 pm, respectively, by means of simulations referring to the permittivity on Ti by using Fresnel equation [18]. These thickness changes were within the 5-nm (=5000 pm) range of the Ti sensing film of the biosensor.

The amount of pH1.9-P-Ser adsorbed onto the biosensor was greater than that of pH 2.0-P-Thr, although the values were not statistically different ($P > 0.05$). The adsorbed amount of pH 1.9-P-RGD was significantly greater than that of pH 3.0-P-RGD ($P < 0.05$), the former value being about 3.6 times as much as the latter. These biomolecules with the phosphate functional group naturally adsorbed onto the oxidized Ti surface as a consequence of the bonding and dissociation mechanism of this functional group. Furthermore, the control of pH played a very important role in the interaction between the biomolecules and Ti surfaces. The point of zero charge (PZC) [19, 20] is an important interfacial parameter used extensively in characterizing the ionization behavior of a surface. The pH at the PZC (pH_{pzc}) depends on material characteristics and influences the base potential. The range of pH_{pzc} for Ti dioxide was 5.6–5.8 at 25°C, and the pH_{pzc} of anatase was slightly higher than that of rutile [20]. The surface potential of Ti dioxide is positively charged when the pH is lower than the pH_{pzc} , whereas the phosphate functional group is negatively charged. Therefore, in this study it was assumed that the phosphate functional group chemically bonded to the oxidized Ti surface. Such a phenomenon coincides with a report on the chemical bond between tantalum and octadecylphosphoric acid [21]. Thus the phosphorylation of molecules may serve to facilitate a stable biochemical modification of the Ti surface, and pH control may promote progressive binding of biomolecules with the phosphate functional group to the modified surface.

Table 1 SPR angle shifts (mDa) at 40 min for each of the H_3PO_4 solutions at pH values of 3.0, 2.0, 1.9, and 1.8

pH	SPR angle shift (mDa)
3.0	6.2 ± 4.6^a
2.0	-32.0 ± 4.0^a
1.9	-48.7 ± 12.6^a
1.8	-125.4 ± 35.8

^a These values were statistically different from that at pH 1.8 ($P < 0.05$)

Fig. 1 Forty-minute time evolution curves during **a** pH 2.0-*o*-phospho-L-threonine adsorption on the Ti-SPR biosensor (*a* solid line) and exposure to pH 2.0-H₃PO₄ as the baseline solution (*a* dotted line), **b** pH 1.9-*o*-phospho-L-serine adsorption on the biosensor (*a* solid line) and exposure to pH 1.9-H₃PO₄ (*a* dotted line), **c** pH 3.0-RGDS(PO₃H₂)PA peptide adsorption on the biosensor (*a* solid line) and exposure to pH 3.0-H₃PO₄ (*a* dotted line), and **d** pH 1.9-RGDS(PO₃H₂)PA peptide adsorption on the biosensor (*a* solid line) and exposure to pH 1.9-H₃PO₄ (*a* dotted line). The SPR angle shift (mDa) was followed during these processes

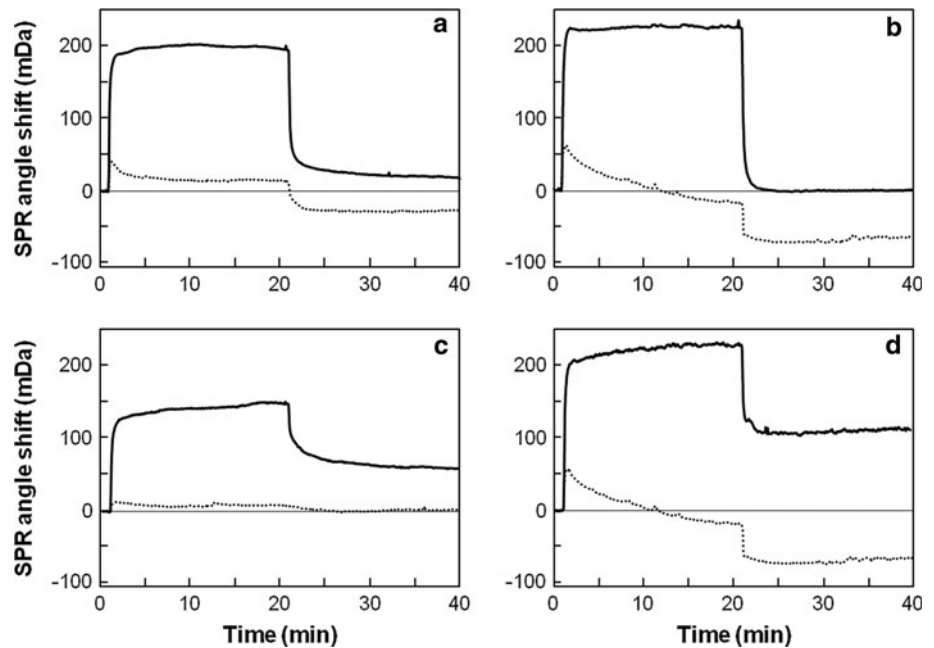


Table 2 Actual SPR angle shift (mDa) and adsorbed amount (pg/mm²) at 40 min for *o*-phospho-L-serine, *o*-phospho-L-threonine and RGDS(PO₃H₂)PA peptide

Compound	pH	SPR angle shift (mDa)	Adsorbed amount (pg/mm ²) ^a
50 mM <i>o</i> -phospho-L-threonine	2.0	32.7 ± 12.8 ^b	131.5 ± 62.9 ^b
50 mM <i>o</i> -phospho-L-serine	1.9	36.6 ± 9.8 ^b	146.9 ± 48.3 ^b
5 mM RGDS(PO ₃ H ₂)PA peptide	3.0	35.7 ± 22.3 ^c	143.3 ± 109.9 ^c
5 mM RGDS(PO ₃ H ₂)PA peptide	1.9	128.6 ± 40.1 ^c	517.1 ± 197.4 ^c

^a Adsorbed amount (pg/mm²) = 4.02 (pg/mm²/mDa) × actual SPR angle shift (mDa)

^b These values were not statistically different ($P > 0.05$)

^c These values were statistically different ($P < 0.05$)

5 Conclusions

The Ti-SPR biosensor in this study accurately measured the time-dependent process of biomolecule adsorption onto the Ti passivation layer. The oxidized Ti surface was etched when exposed to H₃PO₄ solutions with a pH of 2.0 or below. The amount of pH 1.9-P-Ser adsorbed onto the biosensor was larger than that of pH 2.0-P-Thr ($P > 0.05$). The amount of P-RGD adsorbed at pH 1.9 was approximately 3.6 times as much as that at pH 3.0 ($P < 0.05$). These biomolecules naturally adsorbed onto the oxidized Ti surface as a consequence of the bonding and dissociation mechanism of the phosphate functional group. Furthermore, the control of pH played a very important role in the interaction between the biomolecules and the Ti surface.

Acknowledgments This study was partly supported by a Grant-in-Aid for Scientific Research (no. 21592452) from the Japan Society for the Promotion of Science (JSPS) and the Ministry of Education,

Culture, Sports, Science and Technology (MEXT), Japan (2009–2010).

References

- Xiao SJ, Kenausis G, Textor M. Biochemical modification of titanium surfaces. In: Brunette DM, Tengvall P, Textor M, Thomsen P, editors. Titanium in medicine. Berlin: Springer; 2001. p. 417–55.
- Schliephake H, Scharnweber D. Chemical and biological functionalization of titanium for dental implants. J Mater Chem. 2008;18:2404–14.
- Singh N, Cui X, Boland T, Husson SM. The role of independently variable grafting density and layer thickness of polymer nanolayers on peptide adsorption and cell adhesion. Biomaterials. 2007;28:763–71.
- Geißler U, Hempel U, Wolf C, Scharnweber D, Worch H, Wenzel KW. Collagen type I-coating of Ti6Al4V promotes adhesion of osteoblasts. J Biomed Mater Res. 2000;51: 752–60.

5. Ku Y, Chung CP, Jang JH. The effect of the surface modification of titanium using a recombinant fragment of fibronectin and vitronectin on cell behavior. *Biomaterials*. 2005;26:5153–7.
6. Ferris DM, Moodie GD, Dimond PM, Gioranni CW, Ehrlich MG, Valentini RF. RGD-coated titanium implants stimulate increased bone formation in vivo. *Biomaterials*. 1999;20:2323–31.
7. Schuler M, Owen GRH, Hamilton DW, de Wild M, Textor M, Brunette DM, Tosatti SG. Biomimetic modification of titanium dental implant model surfaces using the RGDSP-peptide sequence: a cell morphology study. *Biomaterials*. 2006;27:4003–15.
8. Elmengaard B, Bechtold JE, Søballe K. In vivo effects of RGD-coated titanium implants inserted in two bone-gap models. *J Biomed Mater Res A*. 2005;75:249–55.
9. Healy KE, Ducheyne P. The mechanisms of passive dissolution of titanium in a model physiological environment. *J Biomed Mater Res*. 1992;26:319–38.
10. Viornery C, Guenther HL, Aronsson B-O, Péchy P, Descouts P, Grätzel M. Osteoblast culture on polished titanium disks modified with phosphonic acids. *J Biomed Mater Res*. 2002;62:149–55.
11. Auernheimer J, Zukowski D, Dahmen C, Kantlehner M, Enderle A, Goodman SL, Kessler H. Titanium implant materials with improved biocompatibility through coating with phosphonate-anchored cyclic RGD peptides. *Chembiochem*. 2005;6:2034–40.
12. Abe Y, Hiasa K, Takeuchi M, Yoshida Y, Suzuki K, Akagawa Y. New surface modification of titanium implant with phospho-amino acid. *Dent Mater J*. 2005;24:536–40.
13. Takeuchi M, Abe Y, Yoshida Y, Nakayama Y, Okazaki M, Akagawa Y. Acid pretreatment of titanium implants. *Biomaterials*. 2003;24:1821–7.
14. Knoll W. Polymer thin films and interfaces characterized with evanescent light. *Makromol Chem*. 1991;192:2827–56.
15. Kretschmann E. Determination of the optical constants of metals by excitation of surface plasma. *Z Phys*. 1971;241:313–24.
16. Hirata I, Morimoto Y, Murakami Y, Iwata H, Kitano E, Kitamura H, Ikada Y. Study of complement activation on well-defined surfaces using surface plasmon resonance. *Colloid Surf B Bio-interfaces*. 2000;18:285–92.
17. Hirata I, Akamatsu M, Fujii E, Poolthong S, Okazaki M. Chemical analyses of hydroxyapatite formation on SAM surfaces modified with COOH, NH₂, CH₃, and OH functions. *Dent Mater J*. 2010;29:438–45.
18. Azzam RMA, Bashara NM, editors. Chapter 4: Reflection and transmission of polarized light by stratified planar structures. In: *Ellipsometry and polarized light*. Amsterdam: North-Holland; 1977. p. 269–363.
19. Chou J-C, Liao LP. Study on pH at the point of zero charge of TiO₂ pH ion-sensitive field effect transistor made by the sputtering method. *Thin Solid Films*. 2005;476:157–61.
20. Kosmulski M. The significance of the difference in the point of zero charge between rutile and anatase. *Adv Colloid Interface Sci*. 2002;99:255–64.
21. Textor M, Ruiz L, Hofer R, Rossi A, Feldman K, Hahner G, Spencer ND. Structural chemistry of self-assembled monolayers of octadecylphosphoric acid on tantalum oxide surfaces. *Langmuir*. 2000;16:3257–71.